Pharmaceutical Sciences and Drug Design
ISSN: 3062-4428
2025, Volume 5, Page No: 64-84

Available online at: www.galaxypub.co/page/journals

Galaxy Publication

Elucidating the Core Functional Component Network and Revealing the Molecular Mechanisms of Longdan Xiegan Decoction in Uveitis Therapy

Santiago Flores[1]*, Mateo Ramos[1]

[1]Department of Biotechnology, Faculty of Chemical Sciences, National University of Córdoba, Córdoba, Argentina.

***E-mail** ✉ santiago.flores.ar@gmail.com

Received: 12 January 2025; **Revised:** 18 April 2025; **Accepted:** 18 April 2025

ABSTRACT

Longdan Xiegan Decoction (LXD) is a well-known traditional Chinese herbal formula with demonstrated inhibitory effects on inflammatory cells involved in uveitis. However, the principal functional component combinations and their underlying mechanisms remain unclear.To identify the key component group (KCG) and explore the potential mechanisms of LXD in uveitis treatment, we applied a network community detection model, functional response space analysis, and a reverse prediction model. The effectiveness of the KCG and the validity of our strategy were subsequently verified through MTT, nitric oxide (NO), and ELISA assays. Within the components-targets-pathogenic genes-disease (CTP) network, combining Huffman coding with a random walk algorithm revealed eight foundational acting communities (FACs) with significant functional relevance. Validation demonstrated that these FACs effectively represent the corresponding C-T network for uveitis therapy. Using a novel node importance calculation method, we constructed the functional response space and identified 349 effective proteins. From this, 54 components were selected and defined as the KCG. Pathway enrichment analysis indicated that KCG targets significantly influenced IL-17, Toll-like receptor, and T cell receptor signaling pathways, which are pivotal in uveitis pathogenesis. Experimental validation showed that key KCG components, quercetin and sitosterol, substantially inhibited nitric oxide production and modulated TNF-α and IFN-γ levels in lipopolysaccharide-stimulated RAW264.7 cells. This study elucidates the multi-component, multi-gene, and multi-pathway pharmacological mechanisms of LXD against uveitis through an integrated pharmacology approach. The findings provide a novel framework for future investigations into the anti-uveitis mechanisms of traditional Chinese medicine.

Keywords: Network analysis, Traditional Chinese medicine, TCM, Foundational acting communities, Uveitis, mechanisms, FACs

How to Cite This Article: Flores S, Ramos M. Elucidating the Core Functional Component Network and Revealing the Molecular Mechanisms of Longdan Xiegan Decoction in Uveitis Therapy. Pharm Sci Drug Des. 2025;5:64-84. https://doi.org/10.51847/89ndNVfK1D

Introduction

Uveitis is an inflammatory condition affecting the retinal vessels, retina, choroid, vitreous body, ciliary body, and iris [1], posing a considerable risk of blindness. Epidemiological surveys in the United States and Europe report an annual incidence of 20–50 million cases and a prevalence of approximately 100–150 million [1]. Blindness caused by uveitis accounts for nearly 10% of all cases of blindness [2, 3], highlighting its substantial impact on patients' quality of life and the heavy burden it imposes on families and society.

The pathogenesis of uveitis remains unclear, complicating clinical management. Conventional Western medicine treatment includes pupil dilators, non-steroidal anti-inflammatory drugs, glucocorticoids, and immunosuppressants, typically used in combination based on the underlying etiology. However, growing evidence indicates that traditional Chinese medicine (TCM) is widely applied to treat complex inflammation-driven diseases, including uveitis [4]. Multiple TCM prescriptions, such as Shaoyao Gancao Decoction, Longdan Xiegan Decoction (LXD), and Qufeng Huoxue pill, are used clinically for uveitis [4]. Among these, LXD [5–9]

has been frequently employed in clinical TCM trials due to its anti-inflammatory, hepatoprotective, and immunomodulatory properties and has been shown to successfully control uveitis in practice. Pharmacological studies demonstrate that LXD can alleviate clinical symptoms of experimental autoimmune uveitis (EAU) in rats, reduce the differentiation of uveal-derived CD4+ T cells, and suppress Th1- and Th17-associated cytokines, including IFN-γ and IL-17 [10], consistent with later experimental results. Moreover, LXD can promote IL-10 secretion and restore immune homeostasis, facilitating recovery from autoimmune uveitis, suggesting that its therapeutic effect may involve modulation of the immune response. Histopathological studies have also shown that LXD protects the iris, ciliary body, retina, and other ocular tissues in EAU rats [11]. Nevertheless, as a complex TCM formula, the main active components of LXD and its molecular mechanisms against uveitis remain poorly understood and warrant further investigation.

LXD consists of ten Chinese herbs: Gentiana scabra Bunge [Gentianaceae] (Longdancao, 6 g), Scutellaria baicalensis Georgi [Labiatae] (Huangqin, 9 g), Gardenia jasminoides J. Ellis [Rubiaceae] (Zhizi, 9 g), Bupleurum chinense DC. [Umbelliferae] (Chaihu, 10 g), Alisma plantago-aquatica subsp. orientale (Sam.) Sam. [Alismataceae] (Zexie, 12 g), Plantago asiatica L. [Plantaginaceae] (Cheqianzi, 9 g), Rehmannia glutinosa (Gaertn.) DC. [Scrophulariaceae] (Dihuang, 20 g), Angelica sinensis (Oliv.) Diels [Umbelliferae] (Danggui, 8 g), Glycyrrhiza uralensis Fisch. ex DC. [Leguminosae] (Gancao, 6 g), and Akebia quinata (Thunb. ex Houtt.) Decne. [Lardizabalaceae] (Mutong, 9 g). This formula is recorded in the Chinese Pharmacopoeia. However, the molecular mechanisms underlying LXD's therapeutic effects remain unclear. Developing strategies to identify the key components of LXD and predict their mechanisms could not only inform targeted uveitis treatments but also enhance our understanding of drug–body interactions and guide novel drug discovery.

TCM compound prescriptions are characterized by "multi-target, multi-pathway, and multi-level" effects. In addition, TCM research emphasizes holistic perspectives, syndrome differentiation, and combinatorial prescription use. Network analysis has thus emerged as a powerful tool to overcome limitations of prior pharmacological models and decipher the complex interactions within TCM formulas. This approach leverages the integrity, systematization, and interaction-focused nature of TCM research.

Integrated systems pharmacology has been widely applied to study various disorders. For instance, Gao *et al*. [12] explored the mechanisms of turmeric formula in cardiovascular disease, Bao *et al*. [13] investigated the anti-osteoporotic effects of Xianlinggubao capsule, and Yang *et al*. [14] identified key components and targets of Shengdihuang decoction for dysfunctional uterine bleeding. With the convergence of bioinformatics, integrated pharmacology, and systems biology, along with increasingly accurate computational methods [15–19], integrated systems pharmacology has become a robust framework for elucidating key component groups and mechanisms of TCM prescriptions at the molecular level.

Despite the widespread clinical application of TCM prescriptions, systematic approaches to uncover their synergistic mechanisms remain limited. In this study, we designed an integrated systems pharmacology model to decode the potential mechanisms of LXD in uveitis therapy, providing a methodological reference for treating complex diseases with TCM.

Specifically, to identify the key functional combined component group and clarify the molecular mechanisms of LXD against uveitis, we employed an integrated optimization strategy combining Huffman coding, a random walk algorithm, and a node importance calculation method to capture the key component group (KCG). First, an active ingredients–targets–pathogenic genes–disease network was constructed, and foundational acting communities (FACs) were obtained using a previously published community detection algorithm, validated through pathogenic gene coverage, functional pathway coverage, and key node contributions. Next, a novel node importance method was used to define the key response space and identify effective proteins in FACs, from which the KCG was detected based on the CCR model. Finally, the potential mechanisms of LXD in uveitis were inferred through functional analysis and validated in vitro, demonstrating the reliability of the KCG **(Figure 1)**. This study introduces a network-based approach for evaluating and selecting TCM strategies for complex diseases.

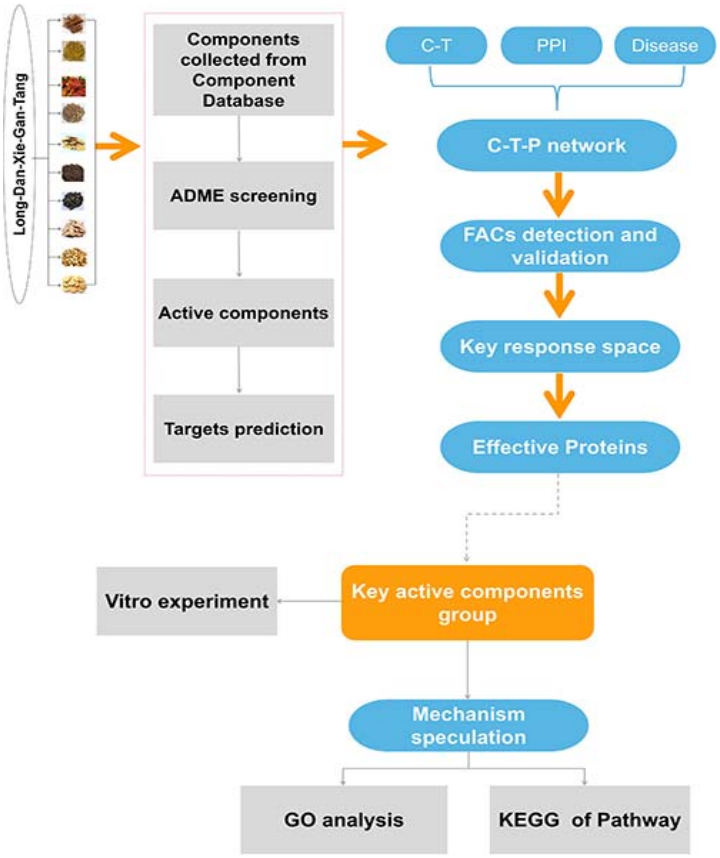

Figure 1. The schematic representation of our proposed network pharmacology strategy. LXD refers to Longdan Xiegan Decoction, and FACs denotes foundational acting communities.

Materials and Methods

ADME screening and active component identification

All chemical constituents of LXD in this study were obtained from the Traditional Chinese Medicine Systems Pharmacology Database (TCMSP, http://lsp.nwsuaf.edu.cn/tcmsp.php) [20]. Since not all constituents possess favorable pharmacological properties, we applied a published ADME model [21] to screen for bioactive compounds. The selection criteria included Lipinski's "rule of five," oral bioavailability (OB, %F) ≥ 30%, and drug-likeness (DL) ≥ 0.14 [22]. Lipinski's rule specifies that a compound's molecular weight (MW) should not exceed 500 Daltons, with the number of hydrogen bond donors, hydrogen bond acceptors, and rotatable bonds not exceeding 5, 10, and 10, respectively, and a logP value between −2 and 5. Oral bioavailability reflects the fraction of an orally administered drug that reaches systemic circulation after gastrointestinal absorption and hepatic metabolism [23]. Drug-likeness describes the physicochemical characteristics that make a compound similar to known drugs [24]. Following ADME screening, 35 potential active ingredients of LXD were identified. Notably, some compounds that did not meet these criteria but demonstrated high concentrations and strong biological activity were also retained as active ingredients.

Network construction

The CTP (components-targets-pathogenic genes-disease) network of LXD was constructed using Cytoscape software [25], and network topology parameters were analyzed with the NetworkAnalyzer plugin [26].

Detection of FACs and effective space

Foundational acting communities (FACs) of LXD for uveitis treatment were identified from the CTP network using a modified version of our previously published mathematical algorithm [27]. The effective space was defined using the following formula:

$$BCCC \geq Med\left\{min^{2}\sqrt{(\sum_{s\neq v\neq t\in V}\frac{\sigma_{vt(s)}}{\sigma_{vt}})\times\sum_{v\neq x}\frac{1}{d(v.x)}}:max^{2}\sqrt{(\sum_{s\neq v\neq t\in V}\frac{\sigma_{vt(s)}}{\sigma_{vt}})\times\sum_{v\neq x}\frac{1}{d(v.x)}}\right\} \quad (1)$$

Med, Min, and Max represent the median, minimum, and maximum values of node importance, respectively.

Here, σvt denotes the total number of shortest paths between nodes v and t, while σvt(s) represents the number of those shortest paths that pass through node s. Nodes xxx and v correspond to genes in the network, and d(v,x) indicates the shortest distance, defined as the minimum number of edges connecting v and xxx.

Cumulative contribution rate of FACs in the CTP network

The contribution weight (CM) reflects the overall net contribution of each FAC within LXD. The R value is used to quantify the influence of individual components, calculated as follows:

$$R=\frac{d_{c}-d_{c}(\min)}{d_{c}\,max-d_{c}\,(min)} \quad (2)$$

$$CC(i)=\frac{\sum_{i}^{n}R_{i}}{\sum_{i}^{n}R_{j}}\times 100\% \quad (3)$$

In this context, dc represents the degree of each component, determined using Cytoscape, while R serves as a measure of the component's influence. Here, n denotes the total number of components in the LXD FACs, and m represents the number of components in the LXD CT network; Ri corresponds to the indicator value for each component in the LXD FACs, and Rj corresponds to the indicator for each component in the LXD CT network.

To construct the CCR model for identifying KCGs: the KCG is embedded within the components of the key response space. The network coverage of each component j in this key response space is denoted as wj, and its contribution rate to pathogenic genes is represented by vj. The maximum expected network coverage of the KCG is given by R. All variables satisfy R>0, wj>0, vj>0, and 1≤j≤n. The task is to select the KCG from the n components in a way that maximizes the cumulative contribution to pathogenic genes. The calculation is formulated as follows:

$$CCR=max\sum_{j=1}^{n}v_{j}\,x_{j} \quad (4)$$

$$\sum_{j=1}^{n}w_{j}\,x_{j}\leq R_{xj}\epsilon\{0,1\},1\leq j\leq n \quad (5)$$

Kyoto encyclopedia of genes and genomes (KEGG) pathway

To investigate the functional roles of FACs, signaling pathways for enrichment analysis were retrieved from the KEGG database [28], with a significance threshold set at $p < 0.05$. The analysis outcomes were visualized using Pathview [29].

Experimental validation

Measurement of NO

Nitric oxide (NO) levels were measured based on our previously reported protocol [27], using quercetin and sitosterol at concentrations of 10–30 μM.

Measurement of TNF-α and IFN-γ

The concentrations of TNF-α and IFN-γ were determined using commercial assay kits according to the manufacturer's instructions.

Statistical analysis

Statistical analyses were performed with SPSS 22.0. Differences among multiple groups were evaluated using one-way ANOVA, and the resulting p-values were adjusted using the Benjamini-Hochberg false discovery rate (FDR). A p-value < 0.05 was considered statistically significant.

Results and Discussion

Chemical analysis

Identifying chemical components is crucial for exploring the active ingredients and mechanisms of Chinese herbal medicines. Through a literature review, the components of LXD with high concentrations and bioactivity were selected. **Table 1** summarizes the chemical constituents of the Chinese herbal medicine along with their concentrations, providing an experimental biochemical framework for identifying potential active compounds.

Table 1. Experimental Chemical Information of Herbs in LXD Based on Published Literature

Herb	Method	Component	Concentration
Gentiana scabra Bunge [Gentianaceae] [Longdancao)	HPLC	Rutin	0.113 mg/g
		Quercetin	0.015 mg/g
		Luteolin	0.011 mg/g
		Kaempferol	0.045 mg/g
		Isorhamnetin	0.021 mg/g
Scutellaria baicalensis Georgi [Labiatae] [Huangqin]	HPLC	Baicalin	122.4 mg/g
		Han-Baicalin	22.25 mg/g
		Baicalein	16.12 mg/g
		Wogonin	4.719 mg/g
		Chrysin	0.3295 mg/g
		Thousand-layer paper element A	3.110 mg/g
Gardenia jasminoides J.Ellis [Rubiaceae] [Zhizi]	HPLC	Geniposidic acid	1.05 mg/g
		Deacetylated methyl oxalate	1.31 mg/g
		Genipin gentian disaccharides	11.40 mg/g
		Geniposide	74.64 mg/g
		Neo-chlorogenic acid	0.25 mg/g
		Chlorogenic acid	2.13 mg/g
		Cryptochlorogenic acid	0.40 mg/g
		Crocin I	0.36 mg/g
Bupleurum chinensie DC. [Umbelliferae] [Chaihu]	HPLC	Saikosaponin a	2.672 mg/g
		Saikosaponin b	1.105 mg/g
		Saikosaponin c	2.328 mg/g
Alisma plantago-aquatica subsp. orientale (Sam.] Sam. [Alismataceae] (Zexie)	HPLC	Alisol A	0.189 mg/g
		Alisol F	2.13 mg/g
		24-acetyl Alisol A	0.913 mg/g
		23-acetyl alisol B	0.444 mg/g
Plantago asiatica L. [Plantaginaceae] (Cheqianzi)	HPLC	Geniposidic acid	21.062 mg/g
		Caffeic acid	0.17 mg/g
		Acteoside	1.58 mg/g
		Isoacteoside	9.38 mg/g
Rehmannia glutinosa (Gaertn.) DC. [Scrophulariaceae]	HPLC	Catalpol	2.113 mg/g
		Acteoside	0.409 mg/g

(Dihuang)			
Angelica sinensis (Oliv.) Diels [Umbelliferae] (Danggui)	HPLC	Ferulic acid	0.36 mg/g
		Coniferylferulate	6.11 mg/g
		Z-ligustilide	4.34 mg/g
		E-ligustilide	0.23 mg/g
		Z-3-butylidenephthalide	0.20 mg/g
		E-3-butylidenephthalide	0.08 mg/g
Glycyrrhiza uralensis Fisch. ex DC. [Leguminosae] [Gancao]	RP-HPLC	Liquiritin apioside	6.33 mg/g
		Liquiritin	35.34 mg/g
		Isoliquiritin apioside	2.21 mg/g
		Isoliquiritin	5.85 mg/g
		Licochalcone B	0.14 mg/g
		Liquiritigenin	0.30 mg/g
		Echinatin	0.10 mg/g
		Isoglycyrrhizin	0.21 mg/g
		Glycyrrhizic acid	121.85 mg/g
Akebia quinata (Thunb. ex Houtt.] Decne. [Lardizabalaceae] (Mutong)	HPLC	Aristolochic acid A	2.73 mg/g

Active components in LXD

A total of 1,278 chemical constituents from 10 different Chinese herbal medicines in LXD were identified through the TCMSP database. Traditional Chinese medicine formulations typically comprise multiple ingredients, and the ADME screening method is commonly applied to select bioactive compounds. Following ADME evaluation, 195 active components in LXD met the comprehensive screening criteria. Further analysis **(Figure 2)** revealed that 10 of these active components are shared by two or more of the constituent herbal medicines.

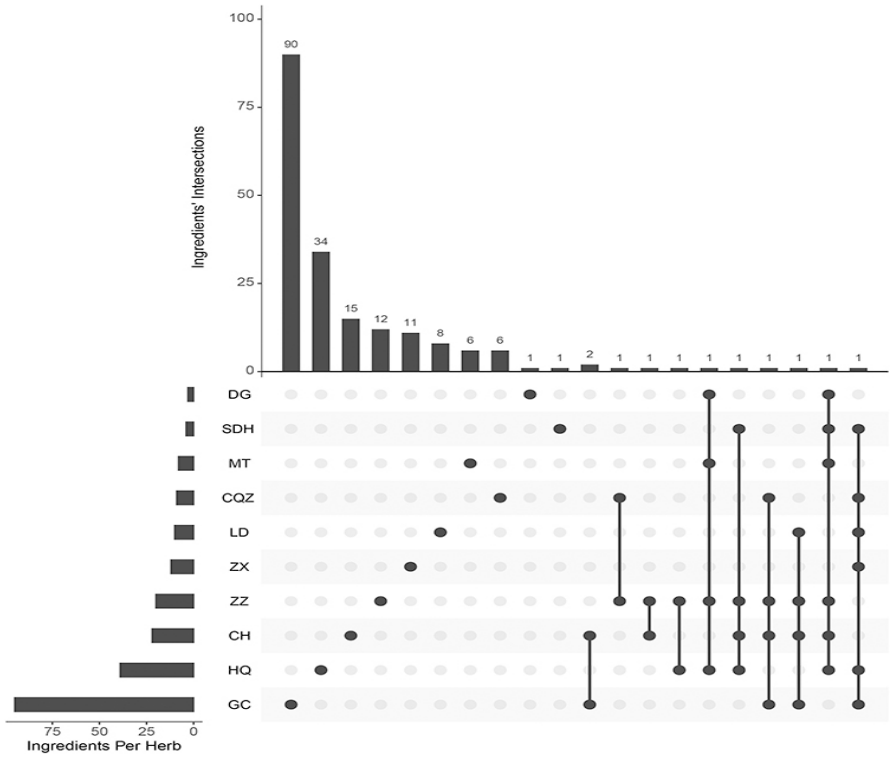

Figure 2. Distribution of active compounds among the herbs in LXD: DG (Angelica sinensis (Oliv.) Diels), SDH (Rehmannia glutinosa (Gaertn.)), MT (Akebia quinata (Thunb. ex Houtt.) Decne.), CQZ (Plantago asiatica L.), LD (Gentiana scabra Bunge), ZX (Alisma plantago-aquatica subsp.), ZZ (Gardenia jasminoides J. Ellis), CH (Bupleurum chinense DC), HQ (Scutellaria baicalensis Georgi), and GC (Glycyrrhiza uralensis Fisch. ex DC).

Weighted gene regulatory network construction in uveitis

The development of uveitis is driven by complex multi-gene interactions, making the creation of a weighted gene regulatory network essential for understanding its underlying mechanisms and guiding therapeutic strategies. Initially, protein-protein interaction (PPI) networks were constructed using data from BioGRID (https://thebiogrid.org/) and STRING (https://cn.string-db.org/). From GeneCards (https://www.genecards.org/), 995 pathogenic genes with associated correlation scores were retrieved. Genes with correlation scores above the median were considered high-confidence, resulting in 767 genes that were mapped onto the PPI network to establish a weighted regulatory network. This network included 704 nodes connected by 36,636 edges **(Figure 3)**. Notably, genes such as CDH1, APC, BRCA2, and MLH1 had correlation scores exceeding 100. While direct evidence linking these genes to uveitis is lacking, prior studies indicate that CDH1 deletion in mice predisposes them to prostatic and chronic uterine inflammation [30, 31], and MLH1 expression rises significantly in chronic gastritis caused by Helicobacter pylori [32]. These observations demonstrate that the weighted network and its prioritized genes provide a meaningful framework for interpreting uveitis pathogenesis and serve as a robust basis for subsequent CTP network construction.

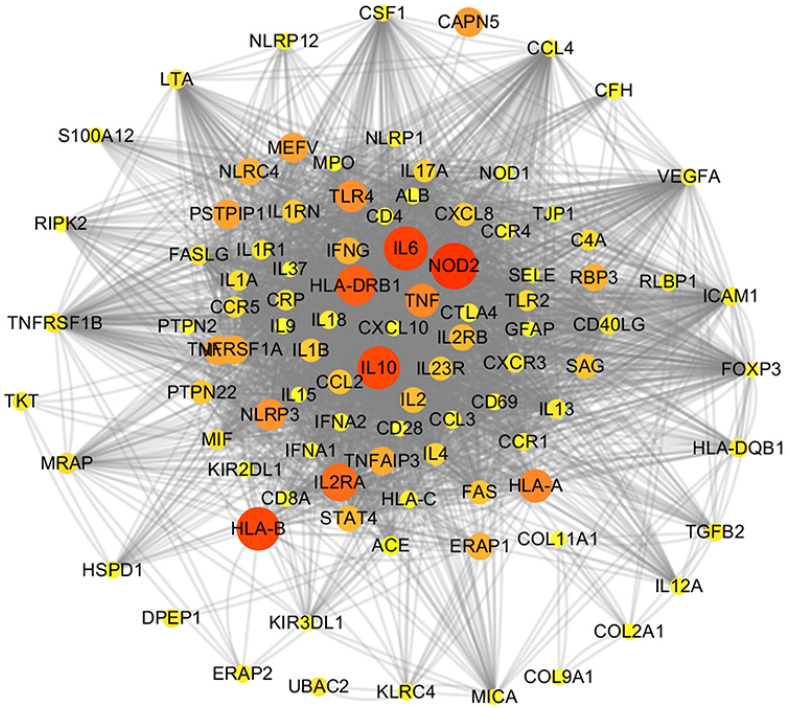

Figure 3. Weighted network of pathogenic genes. The size of each node reflects the gene's weight, and the colors indicate varying node scores.

Construction of the component–target–pathway (CTP) network

To explore the interactions between active compounds in LXD and their corresponding targets, a component-target (CT) network was generated using Cytoscape. The resulting network comprises 195 active compounds, 905 target proteins, and 8,754 interactions. Analysis of network topology with NetworkAnalyzer revealed average degrees of 44.82 for components and 9.68 for targets, indicating that multiple components can regulate a single target, and each component can influence multiple genes. Subsequently, the disease-weighted gene regulatory

network was integrated with the CT network and mapped onto the PPI network, producing the CTP network, which consists of 5,525 nodes and 126,687 edges.

Prediction and validation of FACs

FACs prediction

The CTP network, encompassing both pathogenic and target genes, provides a framework for identifying key drug effect modules essential to understanding LXD's therapeutic mechanisms in uveitis. In this study, a combination of random walk and Huffman encoding-based information mapping algorithms was applied within an integrated systems pharmacology model. This approach identified eight FACs with substantial functional significance within the CTP network **(Figure 4)**.

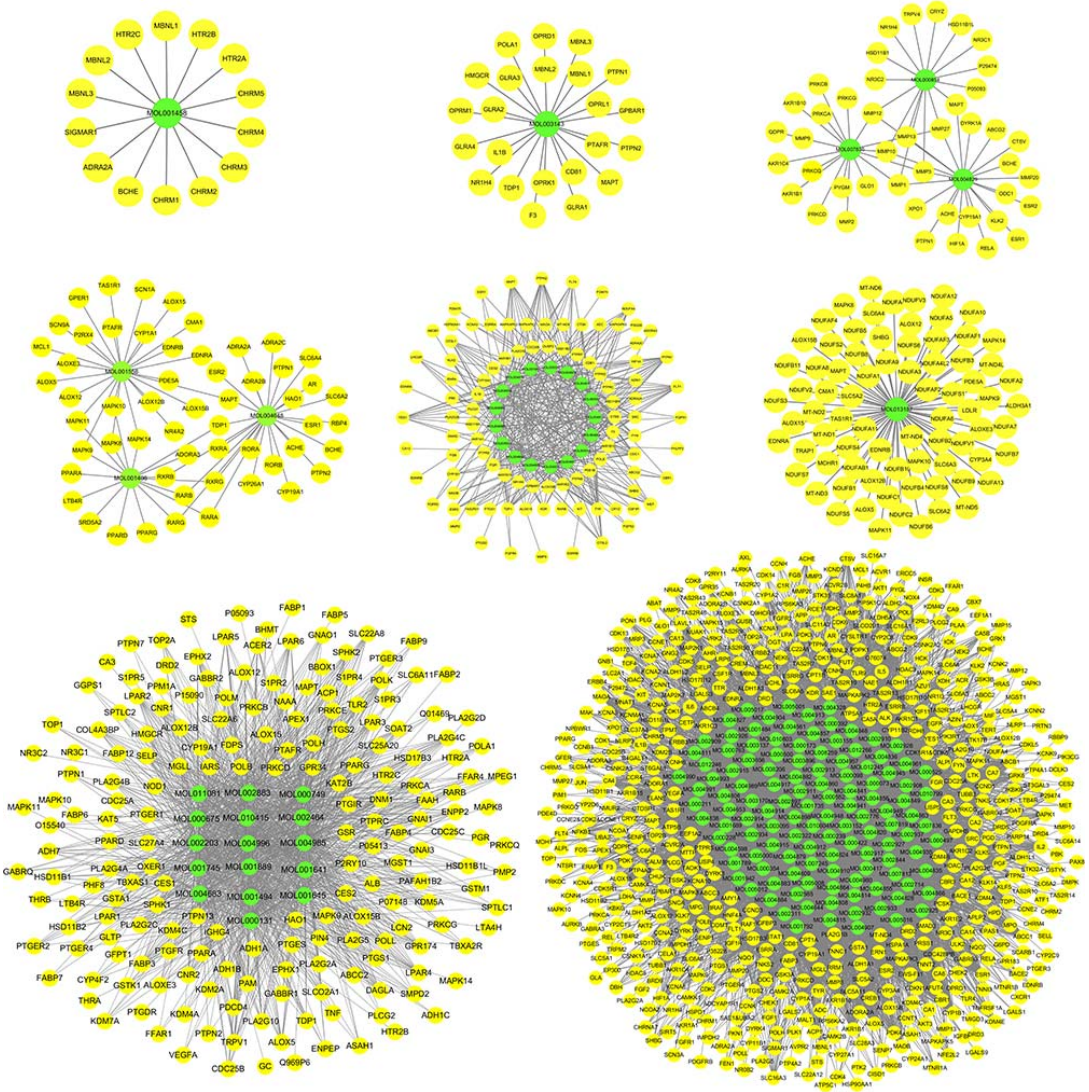

Figure 4. Predicted FACs within the LXD CTP network are shown, where green nodes represent specific LXD components and yellow nodes correspond to their associated targets.

Validation of FACs

To assess whether the predicted FACs accurately represent the C-T network relevant to uveitis treatment, several validation strategies were applied. First, the proportion of pathogenic genes present in the FACs relative to the total pathogenic genes in the CTP network was calculated; a higher ratio indicates that the FACs effectively retain the key pathogenic genes from the full network. Second, the overlap in gene enrichment pathways between the

FACs and the CTP network was examined. Third, the cumulative contribution of critical nodes in the FACs was compared with that of nodes in the entire CTP network; a higher percentage demonstrates that the FACs preserve the most significant nodes of the network.

Comparison of pathogenic gene numbers in FACs and CTP network

To determine how well FACs capture uveitis-associated pathogenic genes, validated pathogenic genes were collected from the literature for analysis. The LXD CTP network contained 20 pathogenic genes, while the FACs included 19 of these genes. This corresponds to a 95% coverage of pathogenic genes within the FACs, indicating strong overlap with the CTP network **(Figure 5)**. These findings demonstrate that the predicted FACs closely match the CTP network in terms of pathogenic gene representation and confirm the reliability and accuracy of the FACs prediction model.

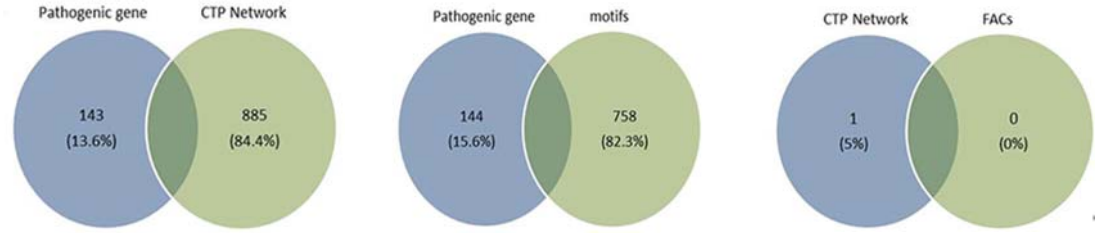

a) b) c)

Figure 5. The overlap of pathogenic genes between the CTP network and FACs in LXD is illustrated using Venn diagrams (a–c), showing the shared gene numbers between the two networks.

Validation of gene enrichment pathways in FACs and CTP network

Functional coherence, reflected by gene enrichment pathways, serves as another measure of the representativeness and impact of predicted communities [33]. In this study, this approach was applied to assess whether the FACs identified in LXD capture the functional characteristics of the complete CTP network. Results indicated that 91.2% of the gene enrichment pathways in the LXD FACs were shared with the full CTP network **(Figure 6)**, demonstrating a high degree of functional overlap. These findings further confirm that the FACs accurately reflect the functional properties of the CTP network, supporting the reliability and validity of the FACs prediction model.

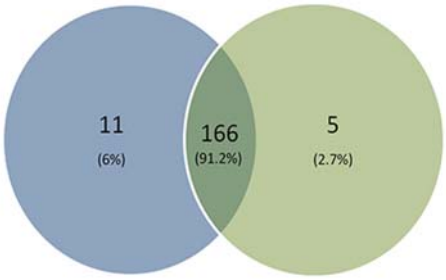

a)

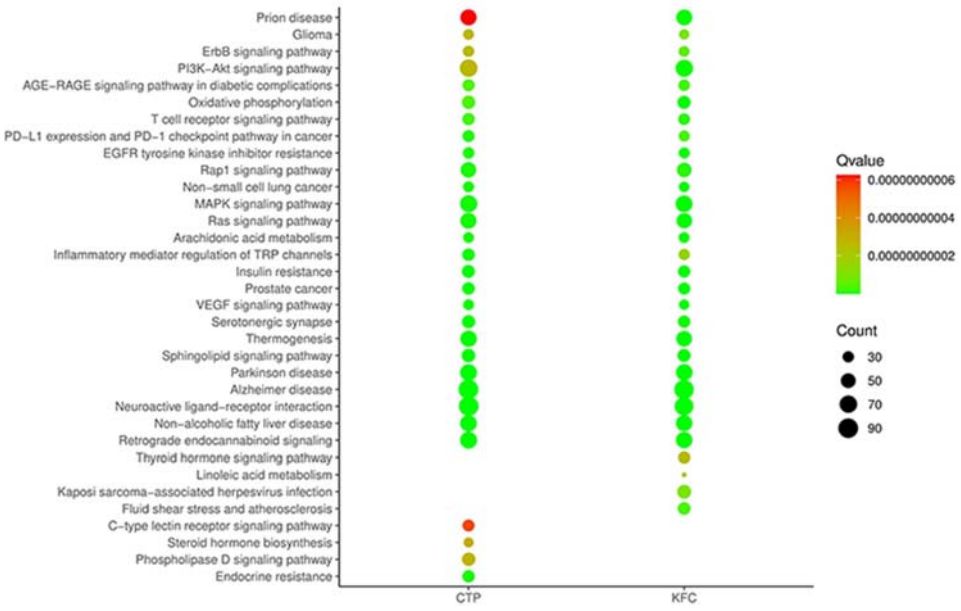

b)

Figure 6. Validation of FACs is presented with (a) a Wayne diagram illustrating the overlap between FACs target genes and the gene enrichment pathways of the CTP network, and (b) a bubble chart displaying the top 30 enriched pathways for both FACs targets and CTP network genes.

Validation of key nodes in FACs and CTP network

Node importance is a critical topological metric for assessing the influence of elements within a network [27]. Using a previously published mathematical model, the significance of nodes in both FACs and the CTP network was evaluated. Each FAC was assigned an R value reflecting its contribution, as detailed in **Figure 7**. Collectively, the eight FACs account for 92.19% of the cumulative contribution observed in the full CTP network, indicating that this approach effectively captures the most influential topological structures within the network.

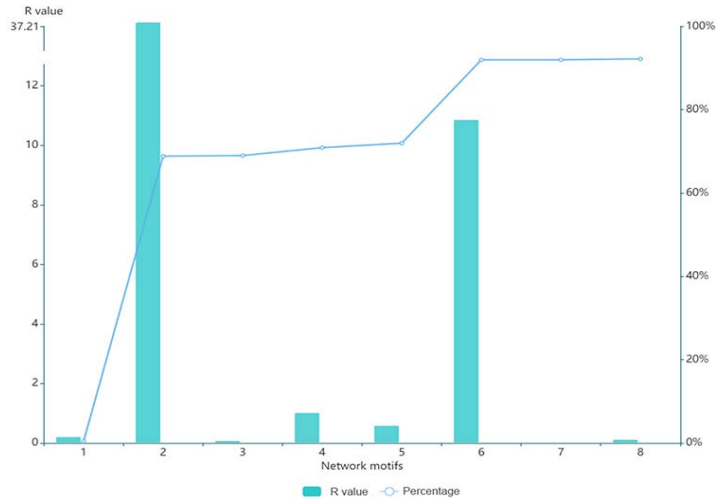

Figure 7. The contribution coefficients of network topology between the C-T network and FACs in LXD are illustrated using a bar diagram, showing the cumulative contribution rate of FACs relative to the full C-T network.

Selection and validation of Effective proteins from key functional communities

Drug action begins with interactions between compounds and cellular components, involving multiple proteins and sometimes genes, forming highly complex networks. The development of many diseases is governed by gene transcription, translation, and protein interactions, which constitute intricate networks that remain incompletely understood. The therapeutic effects of drugs often arise from their active components targeting single or multiple nodes within these networks, ultimately influencing the system as a whole. Node significance is a critical factor in optimizing network interventions. Traditional metrics for evaluating node importance—such as degree, betweenness, neighborhood connectivity, and shortest path—capture only specific aspects of network topology.

In this study, we developed a novel method to calculate node importance based on key functional communities, integrating both node influence and closeness centrality. Using this approach, 349 Effective Proteins were identified from the key functional communities.

To assess the accuracy and reliability of this method, we compared it with conventional node importance measures. The enrichment of LXD target genes and pathogenic genes was analyzed using KEGG and Gene Ontology (GO), and the intersections were considered as primary intervention pathways and GO terms. Using our method, the 349 Effective Proteins accounted for 97.73% of KEGG interventions and 93.67% of GO interventions **(Figure 8c)**. By contrast, Effective Proteins derived from conventional methods—including degree, betweenness, and neighborhood connectivity—showed lower coverage in both KEGG and GO enrichment analyses **(Figures 8a, 8b and 8d).**

These results demonstrate that our key functional community-based method achieves higher accuracy and broader functional coverage than traditional approaches. They also confirm that the identified Effective Proteins play critical roles in the pathogenesis of uveitis.

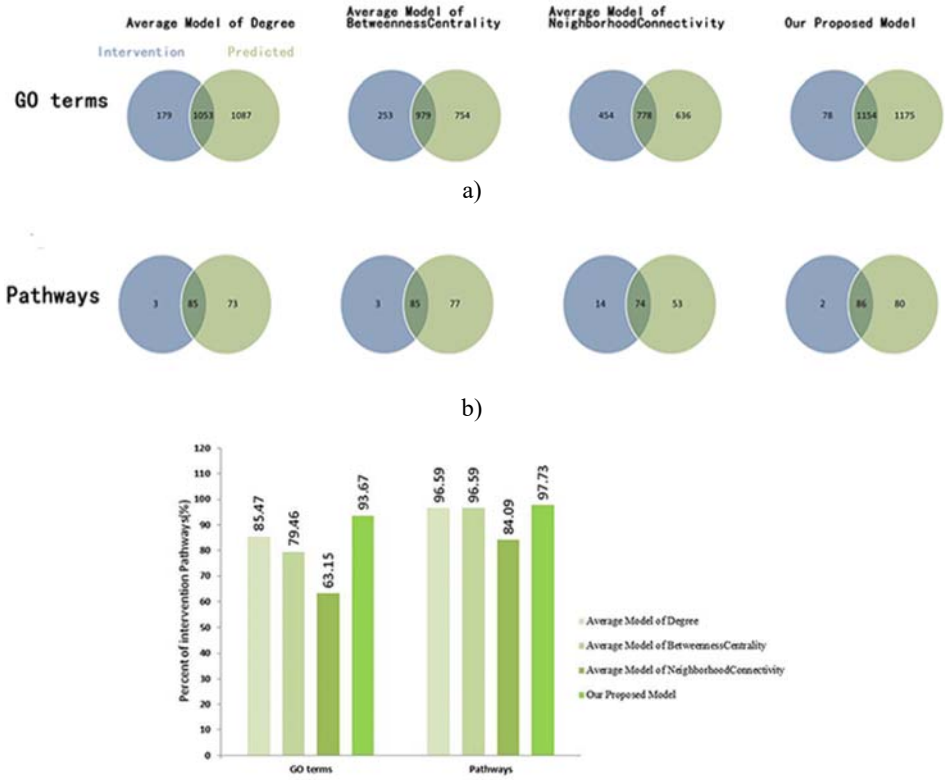

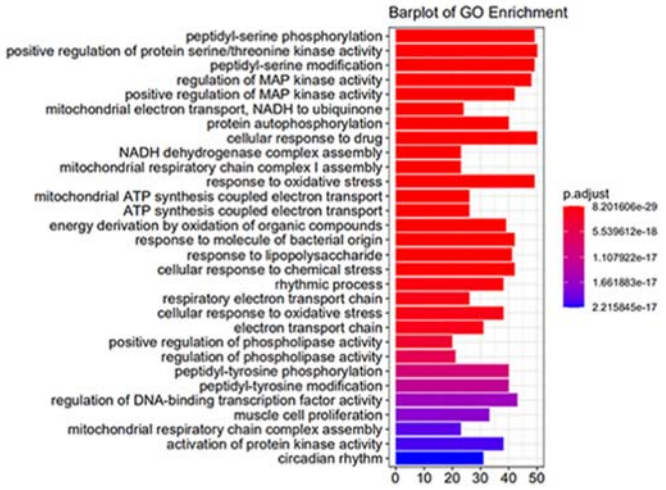

d)

Figure 8. Comparison of our model with other commonly used approaches: (a) Venn diagram showing overlap between GO terms of the four models and the intervention GO terms; (b) Venn diagram depicting the shared pathways between the four models and the intervention pathways; (c) quantitative comparison of our model versus others in terms of intervention pathways and GO terms; (d) bar plot representing pathway enrichment analysis of the Effective Proteins.

Selection and validation of key component groups

To clarify the molecular mechanisms by which LXD treats uveitis, a CCR model was established to optimize the key response space and identify the key component groups. Based on cumulative contribution analysis, the top 10 components—including LXD3 (Sudan III), LXD4 (Ent-epicatechin; ent-Epicatechin), LXD5 (baicalein; wogonin), LXD20 (sitosterol; sitosterol), LXD45 (sophorin; acacetin), LXD77 (baicalin flavone; Panicolin), LXD90, LXD156 (glycerol; Glycyrin), LXD182 (stigmasterol; Stigmasterol), and LXD185 (epberberine; epiberberine)—accounted for 55.87% of the coverage of effective targets. Expanding the analysis, 47 components covered 90.26%, and 54 components contributed 95.42% of effective protein target coverage. Consequently, these 54 components were defined as the key component group; **(Figure 9)**. The high coverage of effective protein targets indicates that this key component group is likely dominant and collectively contributes to LXD's therapeutic effects in uveitis.

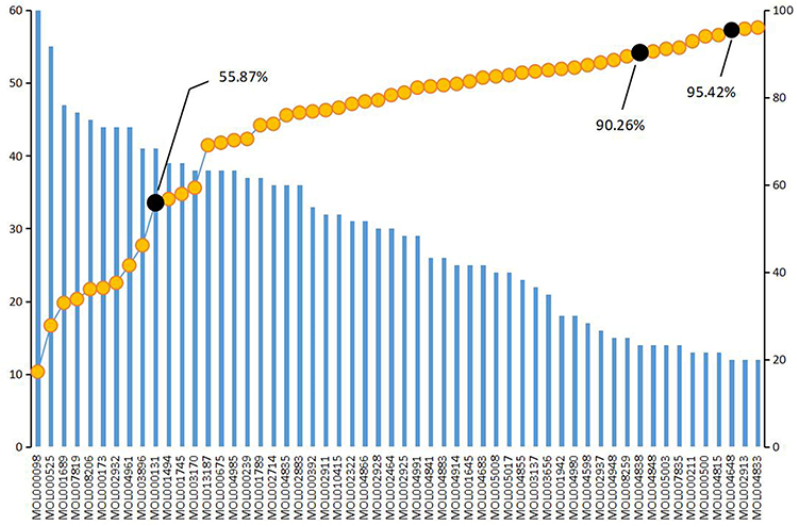

Figure 9. Accumulated contribution scores of active components in LXD are shown.

Functional analysis of LXD in uveitis treatment

To explore LXD's therapeutic mechanisms at the functional level, pathway enrichment analysis was performed using the targets of the key component group and uveitis-associated pathogenic genes. A total of 171 enrichment pathways were identified for the core components ($p < 0.05$) and 116 for pathogenic genes ($p < 0.05$). The pathways associated with the key component group accounted for 77.58% of the pathogenic gene-enriched pathways, highlighting substantial functional overlap. Major enriched pathways included PI3K-Akt (Hsa04151), Ras (Hsa04014), MAPK (Hsa04010), Rap1 (Hsa04015), sphingolipid (Hsa04071), and cAMP signaling (Hsa04024).

For instance, the PI3K-Akt pathway plays a central role in HLA-B27-associated acute anterior uveitis, contributing to anti-inflammatory protection via endotoxin tolerance [34]. Activation of p38 MAPK mediates IL-17(+) uveal T cell responses, exacerbating ocular inflammation in uveitis [35]. Similarly, angiotensin-converting enzyme 2 (ACE2) facilitates the Ras-ACE2/Ang-(1-7)/Mas protective axis, and upregulation of ACE2 mitigates ocular inflammation in experimental autoimmune uveitis (EAU) mice by modulating Th1/Th17 differentiation and M1/M2 macrophage polarization [36].

Sphingolipid metabolites, particularly ceramides, act as bioactive molecules regulating inflammation, with elevated total phospholipids observed in the retinas of endotoxin-induced uveitis (EIU) rats [37]. cAMP, a key second messenger in cellular signaling, has been shown to enhance the therapeutic efficacy of iTregs in EAU when intracellular levels are elevated prior to transplantation [38]. These results support the reliability of combining key reaction networks with CCR modeling to optimize TCM formulations, suggesting that the predicted key component group (KCG) mediates therapeutic effects by modulating T cell proliferation, differentiation, and cytokine secretion.

Potential mechanisms of LXD in uveitis

Uveitis is primarily driven by autoimmune and inflammatory processes, often mediated by Th17 (IL-23/IL-17) and Th1 cells and their cytokines. Analysis revealed 116 pathways shared by the core active component group (CACG) and pathogenic genes, including IL-17 (Hsa04657), Toll-like receptor (Hsa04620), and T cell receptor (Hsa05166) signaling pathways, which are increasingly recognized as relevant to uveitis pathogenesis and therapeutic targets [35, 39, 40].

To systematically map LXD's mechanism, an integrated signaling pathway was constructed using three molecular pathways **(Figure 10)**. In this model, the first three columns represent upstream positions, while subsequent columns indicate downstream targets. The IL-17 pathway (Hsa04657) emerges as a primary target, with LXD modulating 25 upstream targets, including IL-17RA, IL-17RB, IL-17RC, and IL-17RE, and 34 downstream targets, such as IL-6, TNF-α, and MMP3. For the Toll-like receptor pathway (Hsa04620), most LXD-regulated targets, including PKA, AKT, and RAF-1, are positioned downstream. LXD also influences T cell receptor signaling, highlighting its multifaceted role in uveitis therapy. Overall, LXD exerts therapeutic effects by regulating ER-AKT/ERK cascades, synergistically modulating cell cycle progression and promoting apoptosis.

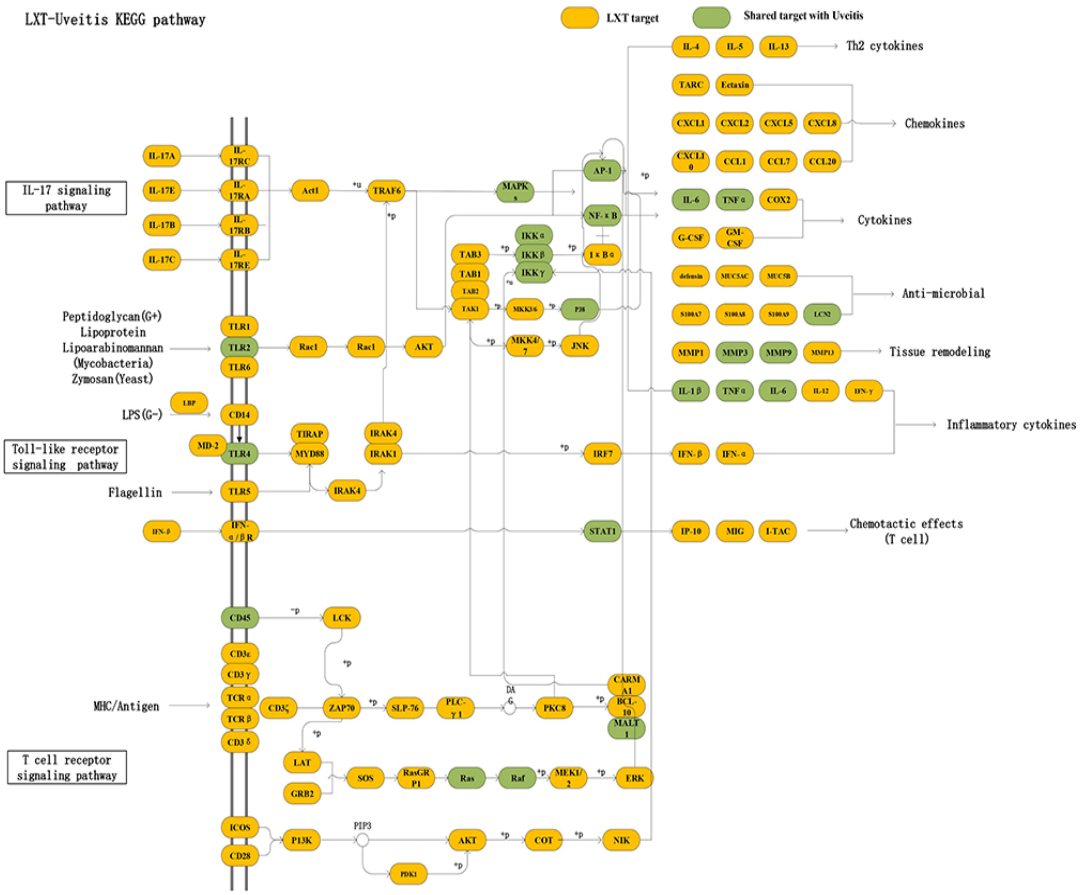

Figure 10. Enrichment pathway map of FACs in LXD associated with uveitis.

In vitro experimental validation of Key component group (KCG)

The impact of quercetin and sitosterol on RAW264.7 cell viability was assessed using the MTT assay. No significant effects on cell viability were observed at concentrations of 10, 20, 30, 40, or 50 μM compared with the control group **(Figures 11a and 11b)**. Based on these results, 10, 20, and 30 μM were selected for subsequent experimental treatments.

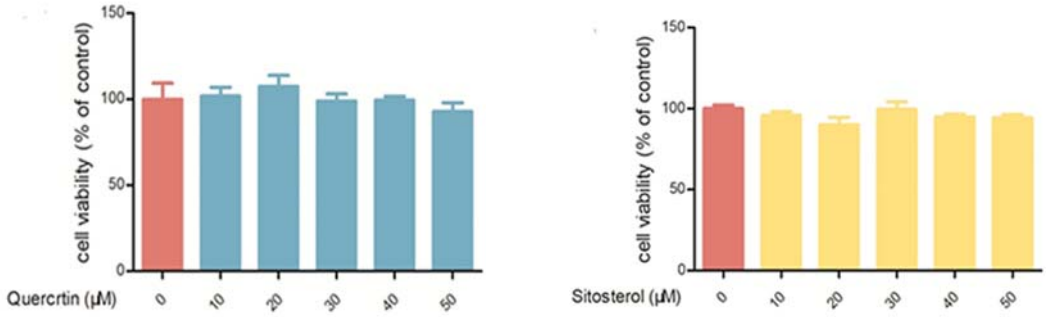

a) b)

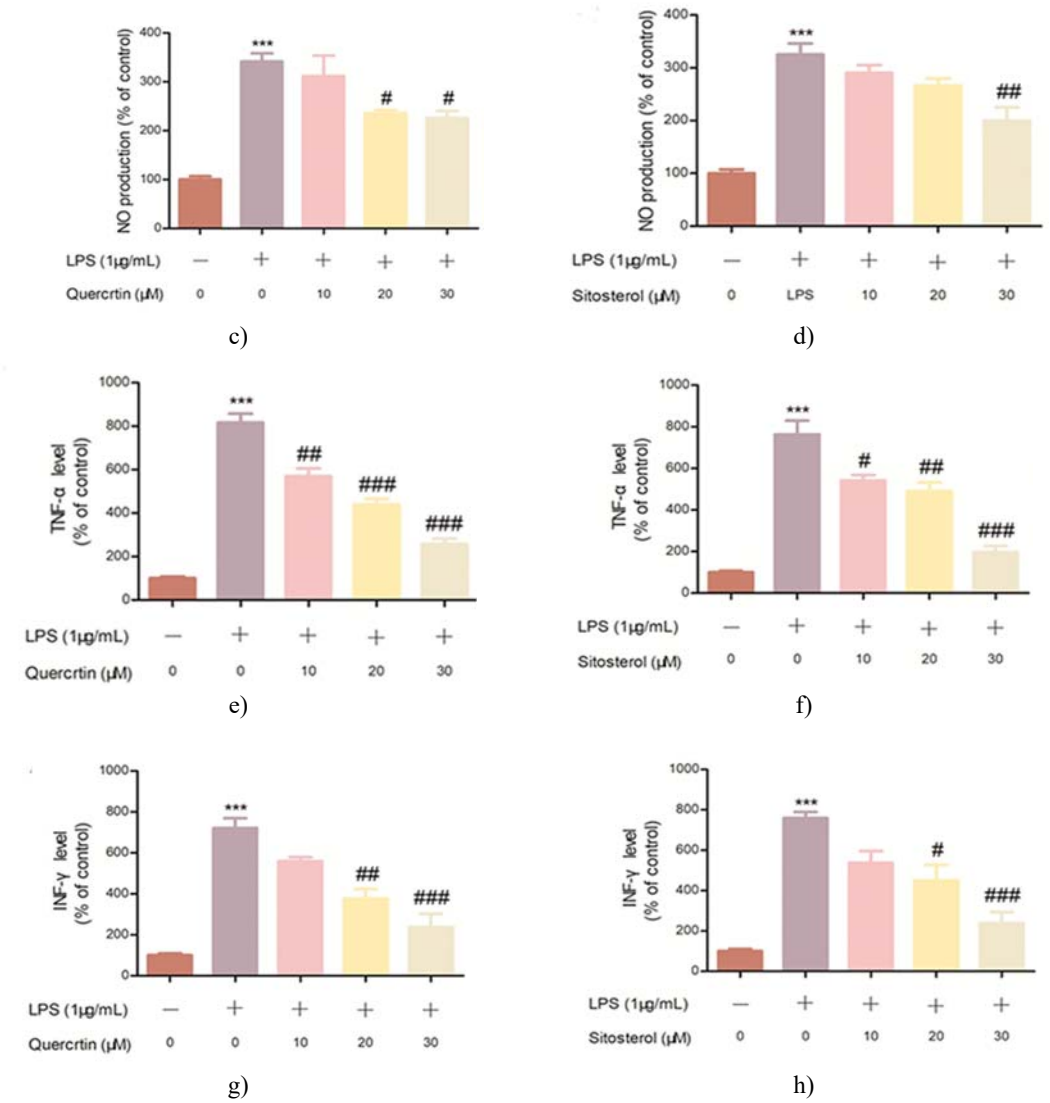

Figure 11. Effects of quercetin (a, c, e, g) and sitosterol (b, d, f, h) on cell viability, NO production, and pro-inflammatory cytokines (TNF-α and IFN-γ) in LPS-stimulated RAW264.7 cells. Statistical significance: ***p < 0.001 vs. control; #p < 0.05, ##p < 0.01, ###p < 0.001 vs. LPS group. Symbols * and # distinguish different comparison groups.

NO functions as an intercellular signaling molecule and plays a critical role in mediating inflammation and immune responses. To validate the predictions of the network pharmacology model, quercetin and sitosterol, key components of LXD, were tested in LPS-induced RAW264.7 macrophages. LPS stimulation increased extracellular NO by 310.90% compared to control, whereas quercetin at 20 and 30 μM reduced NO levels by 77.41% and 86.26%, and sitosterol at 10 and 20 μM decreased NO by 78.43% and 121.84% in a concentration-dependent manner **(Figures 11c and 11d)**. These results indicate that both compounds effectively inhibit LPS-induced NO production.

ELISA assays further demonstrated that LPS markedly elevated TNF-α and IFN-γ levels in RAW264.7 cells: quercetin treatment resulted in increases of 896.24% and 639.40%, and sitosterol treatment produced 764.86% and 802.52% increases relative to control. Pretreatment with quercetin (10, 20, 30 μM) reduced TNF-α levels by 278.19%, 445.19%, and 625.42%, and IFN-γ levels by 117.36%, 283.76%, and 501.63% **(Figures 11e and 11g)**. Sitosterol decreased TNF-α by 274.77%, 228.82%, and 518.46%, and IFN-γ by 267.70%, 500.00%, and 467.70%, respectively **(Figures 11f and 11h)**. These findings are consistent with previous in vivo studies showing that LXD reduces IFN-γ and IL-17 levels, alleviating clinical manifestations of experimental autoimmune uveitis [10].

Conclusion

Current synthetic drugs for uveitis have limited efficacy and often cause adverse effects [41]. In contrast, classical TCM formulations have been used in China for decades, demonstrating notable clinical benefits. At the molecular level, TCM formulas act through multi-component, multi-target, and multi-pathway mechanisms [42–44], making it challenging to elucidate their complex pharmacological actions.

Advances in bioinformatics have facilitated network-based analyses of TCM, allowing the systematic investigation of multi-component interactions and their influence on biological networks [12, 45–48]. These approaches abstract drug-target interactions into networks, enabling the study of drug effects on interconnected biological systems. However, traditional network pharmacology analyses can suffer from redundancy and noise [27]. To address this, we applied an integrated method combining random walk algorithms with Huffman coding to optimize community discovery within CTP networks. This approach, coupled with contribution coefficient modeling, allowed precise identification and validation of functional active communities (FACs) and clarified LXD's mechanism in uveitis.

Following ADME screening, 195 active LXD components were identified. For example, β-sitosterol, present in DG, MT, ZZ, and HQ, downregulates IL-1β, IL-6, and TNF-α, mitigating inflammation. Kaempferol, shared by LD, ZZ, CH, and GC, modulates cytokine secretion and inhibits NF-κB activation. Quercitrin, present in CH and GC, suppresses TNF-α, NO, iNOS, and COX-2 production. Unique components include isoglycyrrhizin from GC, which inhibits TNF-α, IL-6, and IL-4 via NF-κB and MAPK pathways, and aristolochic acid A from SDH, which may exert anti-inflammatory effects by modulating PLA2-mediated arachidonic acid release.

Overall, the combination of network pharmacology, experimental validation, and functional analysis supports that LXD exerts multi-targeted anti-inflammatory effects, providing mechanistic insights into its therapeutic action in uveitis.

To explore the core component group and underlying mechanism of LXD in uveitis therapy, we first predicted the targets of its active ingredients and constructed the corresponding CTP network. Analysis of the network's degree distribution confirmed the multi-target and multi-component characteristics of TCM: individual compounds can interact with multiple genes, and conversely, multiple components can act on the same gene. Nodes with higher degrees are likely to play critical roles in therapeutic effects. For example, quercetin, a widely used dietary flavonoid, exhibits anti-inflammatory activity and significantly reduced inflammation in an S-antigen-induced uveitis rat model [49]. Similarly, 4β→8)-ent-epicatechin demonstrated immunomodulatory properties, highlighting its potential as a candidate for novel immunotherapies [50]. Glabridin exerts anti-inflammatory effects by suppressing cytokine production, inhibiting cyclooxygenase (COX) activity, reducing NO levels, downregulating cGMP, and activating BKCa channels [51]. Several targets such as NODS, IL-6, HLA-B27, and IL2RA showed high nodal degrees. Notably, Blau syndrome, an autoimmune disorder leading to uveitis, is associated with a single amino acid mutation in NODS [52]. IL-6 pathway-targeted therapies are increasingly applied in immune-mediated inflammatory diseases, including uveitis [53], while HLA-B27 and IL2RA are closely linked to acute anterior uveitis and intermediate uveitis, respectively [54, 55]. These findings suggest that advances in genetic engineering could yield more precise treatments for uveitis in the near future.

Biological networks consist of numerous uncertain interactions that collectively form complex regulatory systems. Identifying functional modules within these networks has been a major research focus, giving rise to concepts such as probabilistic network communities, which effectively capture the key functional units involved in disease progression [56]. Detecting motifs and overlapping/non-overlapping communities in networks is critical for understanding their operational principles [57, 58]. Using a network community prediction model, eight FACs were identified in the LXD CTP network. Validation based on pathogenic gene coverage, cumulative contribution of key nodes, and enrichment of functional pathways demonstrated strong concordance with the CTP network, confirming the reliability of our FACs detection strategy.

KEGG enrichment analysis revealed that the therapeutic effects of LXD in uveitis involve the IL-17, T cell receptor, and Toll-like receptor (TLR) signaling pathways. The IL-17 pathway contributes to early uveitic inflammation by promoting cytokine production and recruiting neutrophils, monocytes, and Th1 cells; elevated serum IL-17 is a marker of disease activity [59]. TLRs, key pattern recognition receptors of the innate immune system, detect pathogen-associated molecular patterns, and both preclinical and clinical studies indicate their involvement in uveitis pathogenesis, making them promising therapeutic targets [60]. T-cell-mediated

mechanisms are central to uveitis, and experimental interventions such as the anti-mouse CD3ε antibody Dow2 demonstrate potential for controlling T-cell-driven ocular inflammation.

To identify the key functional response space and effective proteins within FACs, we developed a novel node importance scoring system that considers both connectivity and centrality within the network. Nodes exceeding the median importance score were defined as part of the key response space, and the corresponding proteins were termed effective proteins. This approach maximally reduces network noise. Subsequent functional analyses showed that this method achieved approximately 5% higher accuracy than traditional node scoring methods, further supporting its validity for constructing a functional response space.

Pathway enrichment analysis of the effective proteins revealed their frequent involvement in the PI3K-Akt signaling pathway (hsa04151), MAPK signaling pathway (hsa04010), Ras signaling pathway (hsa04014), and T cell receptor signaling pathway (hsa04660) **(Figure 8d)**. Hoekzema *et al*. reported that endotoxin tolerance, induced by repeated low-dose endotoxin injections, effectively mitigates uveitis in rats, with the PI3K-Akt pathway playing a crucial role in regulating endotoxin-stimulated cytokine expression. Gene expression microarray studies indicate that P13K and Akt are differentially expressed genes potentially central to the pathogenesis of acute anterior uveitis [61, 62]. Jing *et al*. demonstrated that inhibition of the MAPK signaling pathway significantly reduces local inflammation in experimental autoimmune uveoretinitis (EAU) rats, while Huang *et al*. confirmed its anti-inflammatory role in a mouse uveitis model [63–65]. The renin-angiotensin system (Ras), a key hormonal regulator of cardiovascular function, is implicated in several autoimmune diseases, and the protective ACE2/Ang-(1–7)/Mas axis is emerging as a novel target for reducing ocular inflammation [36]. Autoimmune or non-infective uveitis is a vision-threatening intraocular inflammation driven predominantly by T cells, though the contributions of the microbiome and other factors remain incompletely understood [39].

To identify the compounds acting on these key effective proteins, we developed the CCR model, which efficiently extracts key component groups from the functional response space. Subsequent functional analysis and validation of these components indicated that baicalin, a principal active ingredient of LXD, may modulate the T cell receptor signaling pathway to exert therapeutic effects in uveitis. Previous studies have shown that baicalin exerts immunomodulatory effects by activating aromatic receptors, regulating Treg/Teff balance, and controlling CD4+ T cell proliferation, thereby alleviating experimental autoimmune uveitis [66]. Future in vivo studies will further evaluate the accuracy and reliability of our integrated system pharmacology model.

Compared with previous work, our study presents an integrated systems pharmacology strategy that combines Huffman coding, random walk algorithms, node importance scoring, and KCG prediction with validation. This computational approach based on network pharmacology data provides a practical framework to narrow the experimental verification scope. The proposed integrated prediction and validation workflow offers a methodological reference for optimizing core component groups and elucidating the molecular mechanisms of TCM in complex diseases.

Nonetheless, several limitations remain. First, additional components from the key response space should be experimentally validated to further confirm the approach's accuracy. Second, mechanistic predictions from the model, such as the enrichment pathways of key component group targets, require further pharmacological validation both in vitro and in vivo. Finally, the undirected network employed does not capture the activation or inhibitory effects of targets, which limits mechanistic resolution.

Acknowledgments: None

Conflict of Interest: None

Financial Support: None

Ethics Statement: None

References

1. Krishna U, Ajanaku D, Denniston AK, Gkika T. Uveitis: a sight-threatening disease which can impact all systems. Postgrad Med J. 2017;93(1106):766-73. doi:10.1136/postgradmedj-2017-134891

2. Abraham A, Nicholson L, Dick A, Rice C, Atan D. Intermediate uveitis associated with MS: diagnosis, clinical features, pathogenic mechanisms, and recommendations for management. Neurol Neuroimmunol Neuroinflamm. 2021;8(1):e909. doi:10.1212/NXI.0000000000000909
3. Miserocchi E, Fogliato G, Modorati G, Bandello F. Review on the worldwide epidemiology of uveitis. Eur J Ophthalmol. 2013;23(5):705-17. doi:10.5301/ejo.5000278
4. Gao JM, Lyu M, Xie WW, Liu XY, Zhao BC, Zhu Y. Zhong Yi Yao Xin Nao Xue Guan Ji Bing Tong Zhi De Fang Ji Yong Yao Gui Lv Fen Xi. Zhongguo Zhong Yao Za Zhi. 2019;44(1):193-8. Chinese. doi:10.19540/j.cnki.cjcmm.20181101.007
5. Kuang GY. Clinical observation on acute anterior uveitis treated by combination of traditional Chinese and Western medicine. Emerg Tradit Chin Med. 2006;15(7):726-7. doi:10.3969/j.issn.1004-745X.2006.07.029
6. Ning ZC, Chen XH. Research progress of traditional Chinese medicine in the treatment of iridocyclitis. Hebei J Tradit Chin Med. 2020;42(1):151-5. doi:10.3969/j.issn.1002-2619.2020.01.033
7. Pang CS. Experience in the treatment of anterior uveitis. Chin J Tradit Chin Med Ophthalmol. 2004;14(3):52-3. doi:10.3969/j.issn.1002-4379.2004.03.027
8. Xu DM. Treatment of 29 cases of uveitis with combination of traditional Chinese and western medicine. Emerg Tradit Chin Med. 2010;19(4):687. doi:10.3969/j.issn.1004-745X.2010.04.097
9. Yang XH. Professor Lu Mianmian's experience in the treatment of uveitis. Fujian J Tradit Chin Med. 2012;43(2):13,28. doi:10.3969/j.issn.1000-338X.2012.02.008
10. Yin X, Qiu Y, Li Z, Zhang L, Wang Y, Zheng H, et al. Longdan Xiegan Decoction alleviates experimental autoimmune uveitis in rats by inhibiting Notch signaling pathway activation and Th17 cell differentiation. Biomed Pharmacother. 2021;136:111291. doi:10.1016/j.biopha.2021.111291
11. Tang K, Guo D, Zhang L, Guo J, Zheng F, Si J, et al. Immunomodulatory effects of Longdan Xiegan Tang on CD4+/CD8+ T cells and associated inflammatory cytokines in rats with experimental autoimmune uveitis. Mol Med Rep. 2016;14(3):2746-54. doi:10.3892/mmr.2016.5558
12. Gao Y, Wang KX, Wang P, Li X, Chen JJ, Zhou YB, et al. A novel network pharmacology strategy to decode mechanism of Lang Chuang Wan in treating systemic lupus erythematosus. Front Pharmacol. 2020;11:512877. doi:10.3389/fphar.2020.512877
13. Bao H, Guo H, Feng Z, Li X. Deciphering the underlying mechanism of Xianlinggubao capsule against osteoporosis by network pharmacology. BMC Complement Med Ther. 2020;20(1):208. doi:10.1186/s12906-020-03007-1
14. Yang H, Fan Y, Cheng J, Tang Y, Yang F, Li X, et al. Network pharmacology-based prediction of active ingredients and potential targets of ShengDiHuang decoction for treatment of dysfunctional uterine bleeding. Evid Based Complement Alternat Med. 2020;2020:7370304. doi:10.1155/2020/7370304
15. Bhardwaj VK, Oakley A, Purohit R. Mechanistic behavior and subtle key events during DNA clamp opening and closing in T4 bacteriophage. Int J Biol Macromol. 2022;208:11-9. doi:10.1016/j.ijbiomac.2022.03.021
16. Bhardwaj VK, Purohit R. A lesson for the maestro of the replication fork: targeting the protein-binding interface of proliferating cell nuclear antigen for anticancer therapy. J Cell Biochem. 2022;123(6):1091-102. doi:10.1002/jcb.30265
17. Kumar S, Bhardwaj VK, Singh R, Das P, Purohit R. Identification of acridinedione scaffolds as potential inhibitor of DENV-2 C protein: an in silico strategy to combat dengue. J Cell Biochem. 2022;123(5):935-46. doi:10.1002/jcb.30237
18. Singh R, Bhardwaj VK, Das P, Purohit R. Identification of 11β-HSD1 inhibitors through enhanced sampling methods. Chem Commun (Camb). 2022;58(32):5005-8. doi:10.1039/d1cc06894f
19. Singh R, Bhardwaj VK, Purohit R. Computational targeting of allosteric site of MEK1 by quinoline-based molecules. Cell Biochem Funct. 2022;40(5):481-90. doi:10.1002/cbf.3709
20. Ru J, Li P, Wang J, Zhou W, Li B, Huang C, et al. TCMSP: a database of systems pharmacology for drug discovery from herbal medicines. J Cheminform. 2014;6:13. doi:10.1186/1758-2946-6-13
21. Shou WZ. Current status and future directions of high-throughput ADME screening in drug discovery. J Pharm Anal. 2020;10(3):201-8. doi:10.1016/j.jpha.2020.05.004
22. Wang C, Ren Q, Chen XT, Song ZQ, Ning ZC, Lu AP. System pharmacology-based strategy to decode the synergistic mechanism of Zhi-zhu Wan for functional dyspepsia. Front Pharmacol. 2018;9:841. doi:10.3389/fphar.2018.00841

23. Xu X, Zhang W, Huang C, Li Y, Yu H, Wang Y, et al. A novel chemometric method for the prediction of human oral bioavailability. Int J Mol Sci. 2012;13(6):6964-82. doi:10.3390/ijms13066964
24. Tao W, Xu X, Wang X, Li B, Wang Y, Li Y, et al. Network pharmacology-based prediction of the active ingredients and potential targets of Chinese herbal Radix Curcumae formula for application to cardiovascular disease. J Ethnopharmacol. 2013;145(1):1-10. doi:10.1016/j.jep.2012.09.051
25. Demchak B, Hull T, Reich M, Liefeld T, Thompson M, Ideker T, et al. Cytoscape: the network visualization tool for GenomeSpace workflows. F1000Res. 2014;3:151. doi:10.12688/f1000research.4492.2
26. Batt G, Besson B, Ciron PE, de Jong H, Dumas E, Geiselmann J, et al. Genetic network analyzer: a tool for the qualitative modeling and simulation of bacterial regulatory networks. Methods Mol Biol. 2012;804:439-62. doi:10.1007/978-1-61779-361-5_22
27. Wang KX, Gao Y, Lu C, Li W, Zhang Y, Sun Y, et al. Uncovering the complexity mechanism of different formulas treatment for rheumatoid arthritis based on a novel network pharmacology model. Front Pharmacol. 2020;11:1035. doi:10.3389/fphar.2020.01035
28. Kanehisa M, Sato Y, Kawashima M, Furumichi M, Tanabe M. KEGG as a reference resource for gene and protein annotation. Nucleic Acids Res. 2016;44(D1):D457-62. doi:10.1093/nar/gkv1070
29. Luo W, Pant G, Bhavnasi YK, Blanchard SG Jr, Brouwer C. Pathview Web: user friendly pathway visualization and data integration. Nucleic Acids Res. 2017;45(W1):W501-8. doi:10.1093/nar/gkx372
30. Pascal LE, Mizoguchi S, Chen W, Ross AE, Xiao Y, McGrath CM, et al. Prostate-specific deletion of Cdh1 induces murine prostatic inflammation and bladder overactivity. Endocrinology. 2021;162(3):bqaa212. doi:10.1210/endocr/bqaa212
31. Stodden GR, Lindberg ME, King ML, Paechter L, Derocher ME, Giangreco J, et al. Loss of Cdh1 and Trp53 in the uterus induces chronic inflammation with modification of tumor microenvironment. Oncogene. 2015;34(19):2471-82. doi:10.1038/onc.2014.193
32. Bartchewsky W Jr, Martini MR, Squassoni AC, Alvarez MC, Ladeira MS, Ribeiro ML, et al. Influence of Helicobacter pylori infection on the expression of MLH1 and MGMT in patients with chronic gastritis and gastric cancer. Eur J Clin Microbiol Infect Dis. 2009;28(6):591-7. doi:10.1007/s10096-008-0676-2
33. Kanehisa M, Furumichi M, Tanabe M, Sato Y, Morishima K. KEGG: new perspectives on genomes, pathways, diseases and drugs. Nucleic Acids Res. 2017;45(D1):D353-61. doi:10.1093/nar/gkw1092
34. Zhang N, Yu S, Liu X, Lu H. Low dose of lipopolysaccharide pretreatment preventing subsequent endotoxin-induced uveitis is associated with PI3K/AKT pathway. J Immunol Res. 2017;2017:1273940. doi:10.1155/2017/1273940
35. Wei R, Dong L, Xiao Q, Sun D, Li X, Nian H. Engagement of Toll-like receptor 2 enhances interleukin (IL)-17+ autoreactive T cell responses via p38 mitogen-activated protein kinase signalling in dendritic cells. Clin Exp Immunol. 2014;178(2):353-63. doi:10.1111/cei.12405
36. Qiu Y, Tao L, Zheng S, Lin R, Fu X, Chen Z, et al. AAV8-mediated angiotensin-converting enzyme 2 gene delivery prevents experimental autoimmune uveitis by regulating MAPK, NF-κB and STAT3 pathways. Sci Rep. 2016;6:31912. doi:10.1038/srep31912
37. Wang HY, Wang Y, Zhang Y, Wang J, Xiong SY, Sun Q. Crosslink between lipids and acute uveitis: a lipidomic analysis. Int J Ophthalmol. 2018;11(5):736-46. doi:10.18240/ijo.2018.05.05
38. Su W, Chen X, Zhu W, Zhang W, Xu B, Liu X, et al. The cAMP-adenosine feedback loop maintains the suppressive function of regulatory T cells. J Immunol. 2019;203(6):1436-46. doi:10.4049/jimmunol.1801306
39. Horai R, Caspi RR. Microbiome and autoimmune uveitis. Front Immunol. 2019;10:232. doi:10.3389/fimmu.2019.00232
40. Zhong Z, Su G, Kijlstra A, Yang P. Activation of the interleukin-23/interleukin-17 signalling pathway in autoinflammatory and autoimmune uveitis. Prog Retin Eye Res. 2021;80:100866. doi:10.1016/j.preteyeres.2020.100866
41. Urruticoechea-Arana A, Cobo-Ibáñez T, Villaverde-García V, Blázquez-Cañas R, Martín-Martínez MA, Martínez-Ferrer A, et al. Efficacy and safety of biological therapy compared to synthetic immunomodulatory drugs or placebo in the treatment of Behçet's disease associated uveitis: a systematic review. Rheumatol Int. 2019;39(1):47-58. doi:10.1007/s00296-018-4193-z

42. Li DH, Su YF, Sun CX, Fan HF, Gao WJ. A network pharmacology-based identification study on the mechanism of Xiao-Xu-Ming decoction for cerebral ischemic stroke. Evid Based Complement Alternat Med. 2020;2020:2507074. doi:10.1155/2020/2507074
43. Liu Y, Liu Q, Yin C, Li X. Uncovering hidden mechanisms of different prescriptions treatment for osteoporosis via novel bioinformatics model and experiment validation. Front Cell Dev Biol. 2022;10:831894. doi:10.3389/fcell.2022.831894
44. Wu J, Wang K, Liu Q, Li Y, Li X, Li Y, et al. An integrative pharmacology model for decoding the underlying therapeutic mechanisms of Ermiao Powder for rheumatoid arthritis. Front Pharmacol. 2022;13:801350. doi:10.3389/fphar.2022.801350
45. He R, Ou S, Chen S, Ding S. Network pharmacology-based study on the molecular biological mechanism of action for compound Kushen injection in anti-cancer effect. Med Sci Monit. 2020;26:e918520. doi:10.12659/MSM.918520
46. Yang L, Fan L, Wang K, Liu Y, Wu Y, Du Y, et al. Analysis of molecular mechanism of Erxian Decoction in treating osteoporosis based on formula optimization model. Oxid Med Cell Longev. 2021;2021:6641838. doi:10.1155/2021/6641838
47. Zhang Y, Bai M, Zhang B, Liu C, Guo Q, Sun Y, et al. Uncovering pharmacological mechanisms of Wu-tou decoction acting on rheumatoid arthritis through systems approaches: drug-target prediction, network analysis and experimental validation. Sci Rep. 2015;5:9463. doi:10.1038/srep09463
48. Sun J, Liu J, Liu D, Wu X. Network pharmacology-based and clinically relevant prediction of the potential targets of Chinese herbs in ovarian cancer patients. Biomed Res Int. 2020;2020:8965459. doi:10.1155/2020/8965459
49. Romero J, Marak GE Jr, Rao NA. Pharmacologic modulation of acute ocular inflammation with quercetin. Ophthalmic Res. 1989;21(2):112-7. doi:10.1159/000266788
50. Liu Y, Wang C, Dong X, Cheng D, Zhou T. Immunomodulatory effects of epicatechin-(2β→O→7, 4β→8)-ent-epicatechin isolated from Rhododendron spiciferum in vitro. Immunopharmacol Immunotoxicol. 2015;37(6):527-34. doi:10.3109/08923973.2015.1107574
51. Parlar A, Arslan SO, Çam SA. Glabridin alleviates inflammation and nociception in rodents by activating BK(Ca) channels and reducing NO levels. Biol Pharm Bull. 2020;43(5):884-97. doi:10.1248/bpb.b20-00038
52. Parackova Z, Bloomfield M, Vrabcova P, Zentsova I, Filippov S, Sediva A, et al. Mutual alteration of NOD2-associated Blau syndrome and IFNγR1 deficiency. J Clin Immunol. 2020;40(1):165-78. doi:10.1007/s10875-019-00720-6
53. Choy EH, De Benedetti F, Takeuchi T, Hashizume M, John MR, Kishimoto T. Translating IL-6 biology into effective treatments. Nat Rev Rheumatol. 2020;16(6):335-45. doi:10.1038/s41584-020-0419-z
54. D'Ambrosio EM, La Cava M, Tortorella P, Gharbiya M, Campanella M, Iannetti L. Clinical features and complications of the HLA-B27-associated acute anterior uveitis: a metanalysis. Semin Ophthalmol. 2017;32(6):689-701. doi:10.3109/08820538.2016.1170158
55. Lindner E, Weger M, Ardjomand N, Renner W, El-Shabrawi Y. Associations of independent IL2RA gene variants with intermediate uveitis. PLoS One. 2015;10(7):e0130737. doi:10.1371/journal.pone.0130737
56. Ren Y, Ay A, Kahveci T. Shortest path counting in probabilistic biological networks. BMC Bioinformatics. 2018;19(1):465. doi:10.1186/s12859-018-2480-z
57. Ren Y, Sarkar A, Kahveci T. ProMotE: an efficient algorithm for counting independent motifs in uncertain network topologies. BMC Bioinformatics. 2018;19(1):242. doi:10.1186/s12859-018-2236-9
58. Xiang J, Li HJ, Bu Z, Huang C, Li J, Zhang Z, et al. Critical analysis of (Quasi-)Surprise for community detection in complex networks. Sci Rep. 2018;8(1):14459. doi:10.1038/s41598-018-32582-0
59. Jadideslam G, Kahroba H, Ansarin K, Riccardi G, Piccione F, Ghoreishi Z, et al. Interleukin-17 mRNA expression and serum levels in Behçet's disease. Cytokine. 2020;127:154994. doi:10.1016/j.cyto.2020.154994
60. Chang JH, McCluskey PJ, Wakefield D. Recent advances in Toll-like receptors and anterior uveitis. Clin Exp Ophthalmol. 2012;40(8):821-8. doi:10.1111/j.1442-9071.2012.02797.x
61. Booth JW, Telio D, Liao EH, McCaw SE, Matsuzawa T, Gray-Owen SD, et al. Phosphatidylinositol 3-kinases in carcinoembryonic antigen-related cellular adhesion molecule-mediated internalization of Neisseria gonorrhoeae. J Biol Chem. 2003;278(16):14037-45. doi:10.1074/jbc.M211879200

62. Hoekzema R, Murray PI, van Haren MA, Helle M, Kijlstra A. Analysis of interleukin-6 in endotoxin-induced uveitis. Invest Ophthalmol Vis Sci. 1991;32(1):88-95.
63. Huang XT, Wang B, Zhang WH, Peng MQ, Lin D. Total glucosides of paeony suppresses experimental autoimmune uveitis in association with inhibition of Th1 and Th2 cell function in mice. Int Immunopharmacol. 2018;32:394632017751547. doi:10.1177/0394632017751547
64. Jing C, Sun Z, Xie X, Zhang X, Du S. Network pharmacology-based identification of the key mechanism of Qinghuo Rougan Formula acting on uveitis. Biomed Pharmacother. 2019;120:109381. doi:10.1016/j.biopha.2019.109381
65. Wang J, Zhang N, Yu S, Liu XL, Lu H. Effects of endotoxin tolerance on inflammation degree of endotoxin-induced uveitis and PI3K/AKT signaling pathway in iris ciliary body. Yan Ke Xue Bao. 2020;29(1):50-4. doi:10.13281/j.cnki.issn.1004-4469.2020.01.010
66. Zhu W, Chen X, Yu J, Xiao Y, Li Y, Wan C, et al. Baicalin modulates the Treg/Teff balance to alleviate uveitis by activating the aryl hydrocarbon receptor. Biochem Pharmacol. 2018;154:18-27. doi:10.1016/j.bcp.2018.04.006